Environmental Pollution 318 (2023) 120898

Contents lists available at ScienceDirect

Environmental Pollution

journal homepage: www.elsevier.com/locate/envpol

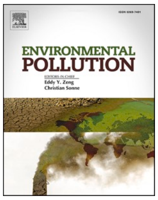

Seasonal variability of phytoplankton community response to thermal discharge from nuclear power plant in temperate coastal area☆

Jingjing Zhang[a,b], Yibin Wang[c,*], Daniel Ottmann[b], Peng Cao[d], Jisong Yang[a], Junbao Yu[a], Zhenbo Lv[a]

[a] *The Institute for Advanced Study of Coastal Ecology, Ludong University, Yantai, 264025, Shandong, PR China*
[b] *Centre for Ocean Life, DTU Aqua, Technical University of Denmark, Lyngby, 2800, Denmark*
[c] *First Institute of Oceanography, Ministry of Natural Resources, Qingdao, 266061, Shandong, PR China*
[d] *Yantai Customs Technology Center, Yantai, 264025, Shandong, PR China*

ARTICLE INFO

Keywords:
Nuclear power plant
Phytoplankton
Seasonal variation
Community structure
Thermal discharge

ABSTRACT

Nuclear power plants (NPPs) developed rapidly worldwide in the last half-century and have become one of the most important electric power sources. Thermal discharge from NPPs increases the temperature of receiving waters, directly and indirectly affecting phytoplankton community. Seasonal and interannual variation in environmental factors in temperate areas makes it challenging to determine the effects of thermal effluents from NPPs on coastal phytoplankton. Here, a five-year study was performed around a NPP in the western Yellow Sea to determine how thermal effluents affect phytoplankton community during different seasons. A total of 106 phytoplankton species from 7 phyla were identified in 10 biological sites during the 19 cruises, among which diatoms dominated phytoplankton abundance in all seasons. Our results show that increased seawater temperature caused by thermal effluents (1) was not enough to cause a statistically significant effect on phytoplankton abundance composition from autumn through spring, (2) significantly stimulated phytoplankton population growth and changed phytoplankton composition in summer (3) increased the proportion of diatoms and decreased the proportion of dinoflagellate in summer, and (4) increased the abundance and dominance of *Skeletonema costatum* sensu lato, especially in summer. The findings of this study provide essential information on the ecological impact of thermal effluents from NPPs in temperate coastal areas.

1. Introduction

Nuclear power plants (NPPs) have become one of the most adopted electrical power sources worldwide due to low carbon emissions and fuel costs (Khan and Nakhabov, 2020). During the last half-century, more than 400 commercial NPPs have been built and operated in 37 countries with a total capacity of 392.61 GW worldwide, which provide approximately 11% of the world's electricity (PRIS, 2021). The long-term threat of global warming, along with the current energy crises, has led to NPPs being reencouraged globally (WNPR, 2022). However, the operation of NPPs requires large amounts of cooling water, thus they are usually located in coastal areas to facilitate the use of seawater as a cooling medium (Poornima et al., 2005). Simultaneously, NPPs generate vast amounts of warm water effluents (Hu, 2004), which significantly elevate the seawater temperature of the surrounding aquatic system (Krishnakumar et al., 1991; Langford, 1990). A study has shown that the difference in temperature between intake water and outlet water can be as high as 7–10 °C (Bamber and Seaby, 2004), which can considerably threaten the ecological environment and aquatic organisms in the coastal bodies (Choi et al., 2002; Lo et al., 2004; Suresh et al., 1993).

As an important primary producer, phytoplankton plays essential roles in the food chain, matter circulation, and energy flow in coastal ecosystems (Field et al., 1998). Thermal discharge from NPPs has the potential to affect phytoplankton survival, growth, and reproduction of the receiving waters (Langford, 1990; Lo et al., 2004; Poornima et al., 2006), thus resulting in the variation of upper trophic levels and the modification of ecosystem. Compared to other organisms, phytoplankton are more sensitive to environmental changes. Even small changes in the physical and chemical properties of water can cause

---

☆ This paper has been recommended for acceptance by Amit Bhatnagar.

* Corresponding author. First Institute of Oceanography, Ministry of Natural Resources, 6 Xianxialing Road, 266061, Qingdao, China.
E-mail address: wangyibin@fio.org.cn (Y. Wang).

https://doi.org/10.1016/j.envpol.2022.120898
Received 3 October 2022; Received in revised form 30 November 2022; Accepted 16 December 2022

significant changes in the phytoplankton community (Behrenfeld and Boss, 2014; Gómez et al., 2011). Therefore, monitoring variations in phytoplankton abundance and composition servees as an essential assessment method for evaluating the impact of thermal effluents on aquatic ecosystems.

Current studies on the effects of thermal discharge on phytoplankton communities in aquatic ecosystems concern mainly tropical areas (Rajagopal et al., 2012). In tropical regions, where ambient seawater temperature is close to the upper tolerance limit for marine algae, a further increase in temperature caused by thermal discharge usually suppresses the growth of phytoplankton around NPPs (Chuang et al., 2009; Ma et al., 2011; Poornima et al., 2012; Suresh et al., 1993). Compared to tropical regions, the impact of thermal discharges on phytoplankton population is more complicated in temperate areas because seasonal variations in environmental variables and phytoplankton composition may contribute to different responses to thermal stress between seasons (Begun and Maslennikov, 2021; Roemmich and McGowan, 1995; Tang et al., 2013). Limited studies have analyzed the effects of thermal discharge on phytoplankton community in temperate areas by comparing the changes in phytoplankton abundance and composition in different regions of the NPPs (Chuang et al., 2009; Lee et al., 2018; Poornima et al., 2005; Xu et al., 2021), or the changes

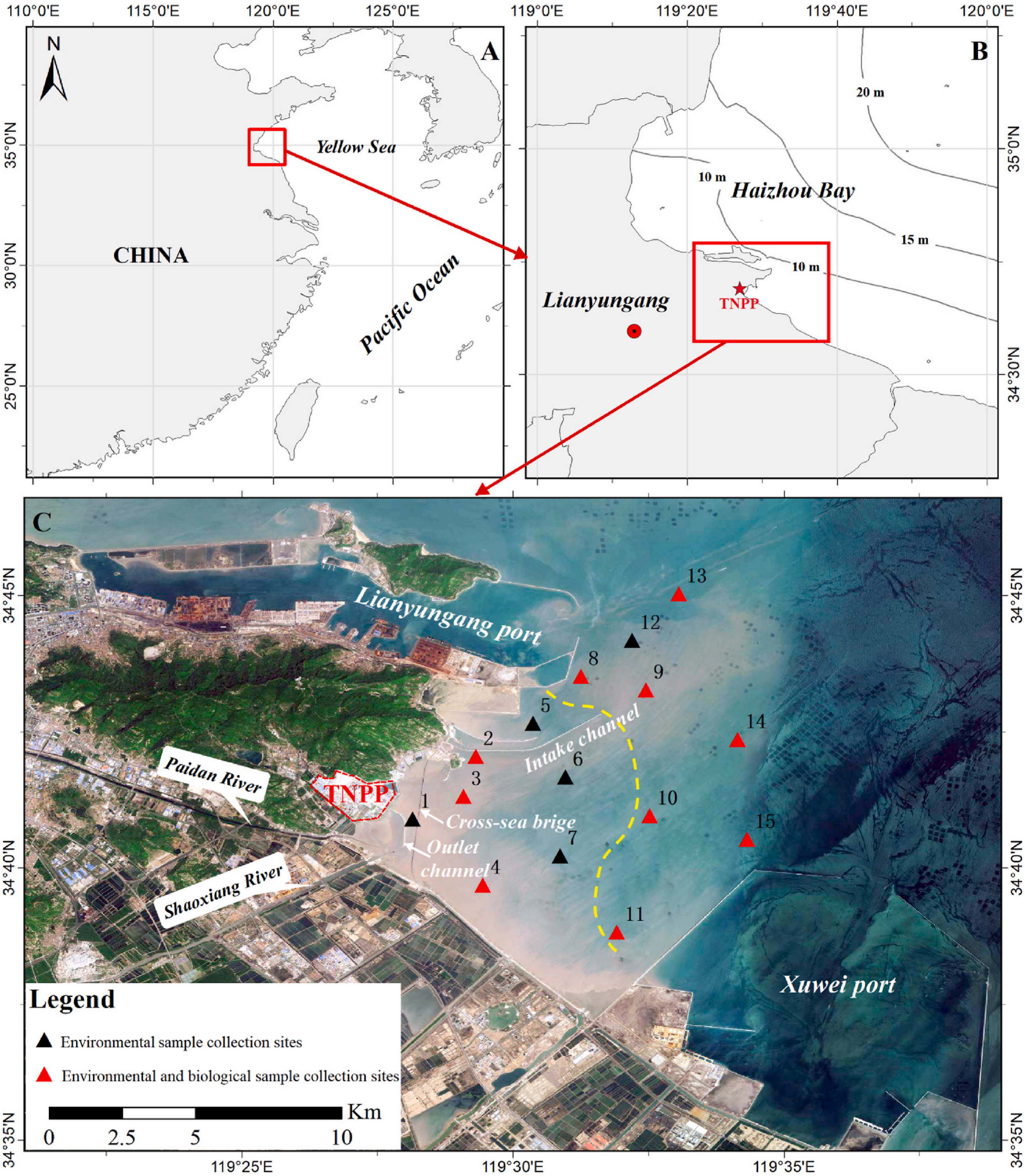

Fig. 1. Study area and sampling sites around Tianwan nuclear plant (TNPP), A: location of the Haizhou Bay and the Yellow Sea, B: location of the Haizhou Bay and Lianyungang City, C: sampling sites. The black triangles indicate that only environmental samples were collected at these sites, while the red triangles indicate that both environmental and biological samples were collected at these sites. The yellow dashed line represents the farthest limit of ≥1 °C temperature rise caused by thermal discharge. Redrawn from (Nie et al., 2021). (For interpretation of the references to color in this figure legend, the reader is referred to the Web version of this article.)

before and after NPPs construction (Lin et al., 2018; Yu et al., 2007), but the results are not consistent. Some studies suggest that the thermal effect on phytoplankton abundance and composition is not statistically significant or localized (Ikäheimonen et al., 1995; Mercado and Gomez, 1999; Poornima et al., 2005). However, other researchers believe that the thermal discharge stimulates phytoplankton growth during cold seasons but inhibits primary productivity during warm seasons (Morgan and Stross, 1969), with more notable effects in cold seasons (Lin et al., 2018; Xu et al., 2021). To date, we do not fully understand the effects of thermal discharge from NPPs on the changes in phytoplankton community during different seasons in temperate areas because previous studies based on the comparison of different regions in a single year or two years in the same area could not exclude the effect of spatial and inter-annual differences in environmental factors on phytoplankton abundance and composition. Therefore, long-term continuous observations, which can effectively reduce random error, are desperately required for accurately assessing potential alterations in the phytoplankton community in temperate areas due to thermal discharge from NPPs.

To accurately assess the effect of thermal effluents from NPPs on the phytoplankton population across seasons in temperate coastal regions, we collected physical, chemical, and biological data in 19 surveys around the coastal area of Tianwan nuclear power plant (TNPP) from February 2011–February 2016. We investigated the spatial distribution of phytoplankton abundance and community composition relative to thermal discharge during different seasons. First, we compared the difference in environmental factors and phytoplankton community between sites inside and outside of the area affected by the thermal effluence of TNPP. Then, we evaluated the effects of thermal effluents on phytoplankton abundance and composition across different seasons. Finally, we constructed regression tree models to distinguish whether phytoplankton differences are due to warming caused by thermal emissions or changes in other environmental factors.

2. Materials and methods

2.1. Study area and sampling sites

Tianwan nuclear power plant (TNPP) lies on the south coast of Haizhou Bay, in the western Yellow Sea (Fig. 1). The coastal area around TNPP is a typical temperate open bay with four distinct seasons, and the surface seawater temperature range from −0.1 °C in February to 29.5 °C in August (Wang and Xiong, 2013). Strong northerly monsoon prevails over the study area during winter with an average wind speed of 10 m/s in January (Yuan and Su, 1984), while southerly wind prevails over the area during summer with an average wind speed of about 1.5 m/s (Mask et al., 1998). The study area is relatively shallow, with water depth ranging from 3 to 13 m (Fig. 1B), making it more sensitive to environmental variability (Liu et al., 2019), and the hydrodynamic process is mainly controlled by the movement of the tide and wind-induced currents (Hu et al., 2013; Huang et al., 2012). Two small ephemeral rivers flow into the study area with an annual mean discharge of 2.63×10^7 m^3 (Wang et al., 2022). More than 70% of water discharge flows into the study area during summer, which makes the water salinity fluctuate between 23.5 and 29.5 during wet season (summer) and 28.5–30.5 during dry season (winter and spring) (Zhang, 2006).

TNPP is consist of 8 reactor units, with a total installed capacity of 8270 MW (PRIS, 2021). TNPP uses a once-through cooling system (Wei et al., 2016), and the thermal discharge from the power plant is constant during the whole seasonal cycle. During 2011–2016, two 1060 MW units (No.1 and No.2) were put into operation, with a flow rate of 120 m^3/s. Thermal water is discharged to the surrounding environment through an open channel, and the water depth around the outlet is less than 3 m (Wang et al., 2022). Affected by the thermal discharge, an apparent temperature rising zone has been observed in the study area since TNPP was put in operation, with influence range increases during ebb tide and decreases during flood tide (Nie et al., 2021; Wang and Xiong, 2013).

In this study, the monitoring program was designed with 15 environmental sampling sites set out in a radial pattern in an area of about 90 km^2 from TNPP. In addition to environmental samples, phytoplankton samples were collected from 10 of the 15 sites (Fig. 1C). Sites 1–7 are located inside the area heated by TNPP ($\geq$1 °C change in water T°), while sites 8–15 are outside the heated area ($<$1 °C change in water T°) (Nie et al., 2021). During February 2011–February 2016, four monitoring cruises were conducted in February (winter), May (spring), August (summer), and November (autumn) each year, except for only summer and autumn cruises in 2013 (Supplementary Table S1). We compared the variation of phytoplankton abundance and composition between the heated (inside) area and the surrounding (outside) control area to determine the effect of thermal discharge on phytoplankton community.

2.2. Environmental factors

Temperature and salinity were measured in situ using a Conductivity-Temperature-Depth/Pressure Profiler (RBRconcerto^3). Surface water samples were collected using Niskin bottle rosette samplers for the detection of nutrients and total suspended matter (TSM). Surface seawater samples for nutrient analysis were filtered using 0.45 μm acetate cellulose filters and immediately preserved at −20 °C in a refrigerator.

The nutrient content of the water samples, including dissolved inorganic nitrogen (DIN), which is the sum of NO_3, NO_2, and NH_4, dissolved inorganic phosphate (PO_4), and dissolved silicate ($Si(OH)_4$), was determined using an autoanalyzer (QuAAtro AutoAnalyzer 39) (Wang et al., 2017). NO_3, NO_2, and NH_4 were measured using the diazo-azo method, cadmium-copper reduction method, and salicylate method, respectively. The concentrations of PO_4 and $Si(OH)_4$ were measured using the phosphomolybdenum blue method and the silicomolybdic complex method, respectively. The detection limits for NO_3, NO_2, NH_4, PO_4, and $Si(OH)_4$ were 0.02, 0.006, 0.03, 0.006, and 0.03 μmol/L, respectively. Water samples (500–1000 mL) for TSM were filtered using dried and pre-weighed Sartorius™ acetate fiber filters with a pore size of 0.45 mm and a diameter of 47 mm, after which they were stored at −20 °C until analysis. TSM was measured by the gravimetric method following the Chinese National Standard GB 17378.4–2007. The filters were dried in an oven at 40 °C for 6–8 h, then transferred into a silicone rubber dryer for 6–8 h to a constant weight. The filter was reweighed, and the weight difference between the reweighed and pre-weighed is the TSM value in mg/L (Zhang et al., 2021).

2.3. Phytoplankton analysis

Surface seawater samples (500 mL) were collected and fixed in formalin solution (4% final concentration) and stored at 4 °C for laboratory taxonomic analysis. Phytoplankton abundance was determined using the Utermöhl method (Utermöhl, 1958). The shaken fixed sample (25 mL) was put into the Utermöhl counting frame and sedimented for 24 h. Then, phytoplankton species were identified and counted under an Olympus CKX53 inverted microscope at 200 × and 400 × magnification, and the cell size limit of identification was approximately 7 μm. The phytoplankton density was calculated by the number of algae cells per liter of seawater (cell/m^3).

Dominant species were determined using the dominance index (Y), and phytoplankton species were considered dominant when $Y \geq 0.02$.

$$Y = \frac{n_i}{N} \times f_i$$

Where n_i is the cell number of the specie i, N is the total number of cells in the sample, and f_i is the occurrence frequency of specie i at all sites.

2.4. Data analysis

Temporal and spatial variations in environmental factors and phytoplankton abundance were mapped. Welch's *t*-test was performed to determine whether phytoplankton abundance and environmental factors differed between sites inside and outside the heated area. Analysis of similarities (ANOSIM) was used to analyze the resemblances in phytoplankton composition between the two areas. Prior to performing the redundancy analysis (RDA), normal distribution of all environmental variables and phytoplankton data were tested with a Pearson's moment coefficient of skewness, and we applied a log $(x+1)$ conversion to variables that did not conform to normal distribution.

RDA was used to determine the effects of environmental factors on the succession of dominant species because of the results of detrended correspondence analysis (DCA) showing the maximum gradient length of the first axis between 3 and 4. Only the species with mean dominance $Y \geq 0.02$ during 2011–2016 were selected for RDA analysis to facilitate the interpretation of results.

The regression tree model is an effective method for determining the control factors (Lofton et al., 2020). Regression trees were constructed to assess the relative importance of thermal discharge and environmental variation controlling phytoplankton community in summer when significant differences in phytoplankton abundance and composition were observed between sites inside and outside of the area heated by the NPP. Before the regression tree analysis, all environmental variables were tested for correlations by applying Spearman's correlation analysis. DIN, with high correlations with PO_4 (Spearman's coefficients $\rho = 0.58$), and $Si(OH)_4$ ($\rho = 0.61$), was excluded to ensure the selected driver variables no strongly correlated. Temperature was selected to represent the effect of thermal discharge, while salinity, TSM, PO_4, and $Si(OH)_4$ represented the effect of environmental variation. Separate regression tree analyses were conducted for phytoplankton and main dominant species, and the reliability of the regression tree models was verified by cross-validation procedure (Lofton et al., 2020).

To further determine whether the significant difference in plankton composition between sites inside and outside the heated area in summer was caused by the thermal discharge, we used regression tree models to predict the abundance of total phytoplankton and dominant species in different sites when water temperature of inside sites was equal to the average temperature of the outside sites and the other environmental

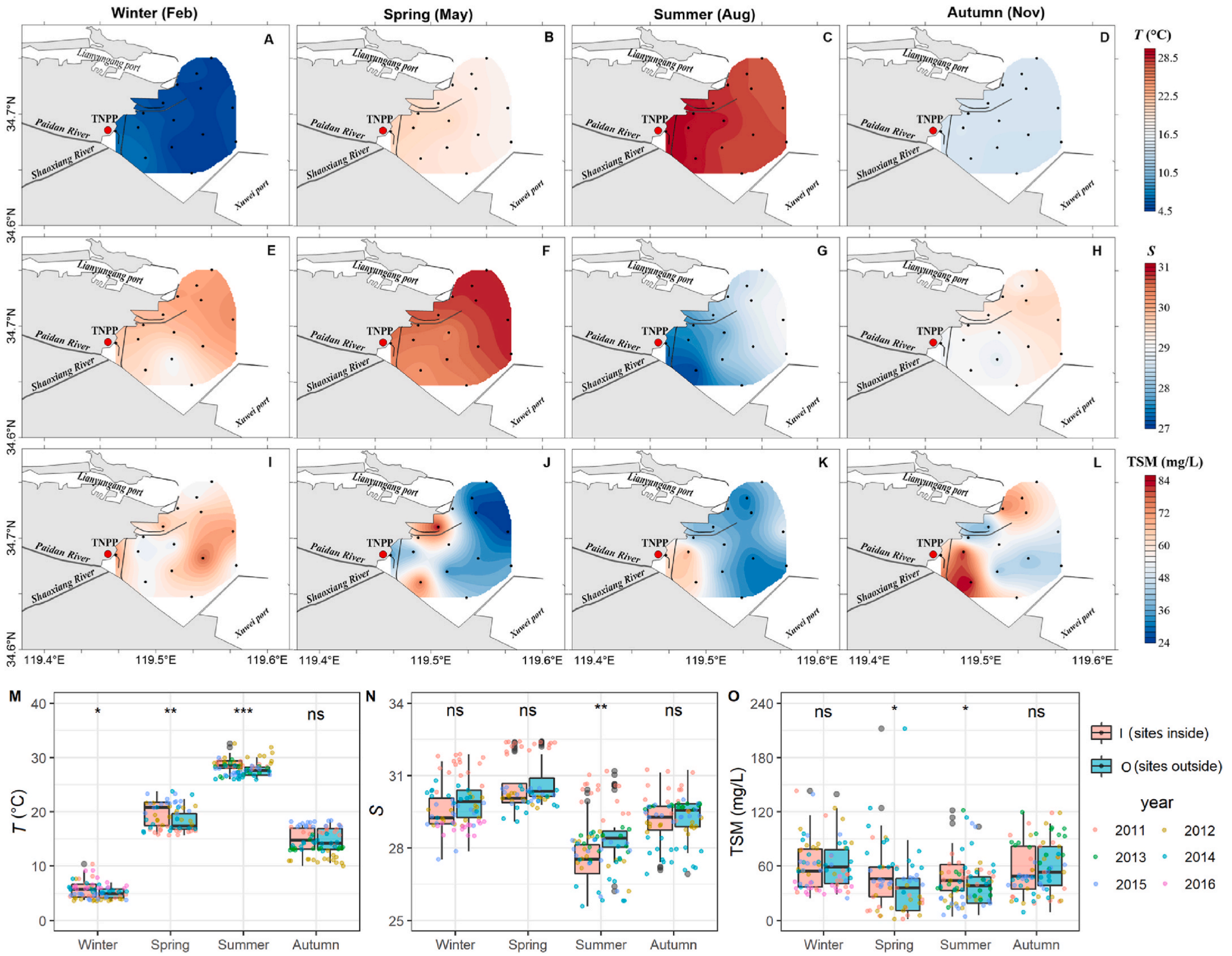

Fig. 2. Spatial and temporal variation of temperature (*T*), salinity (*S*), and total suspended matter (TSM) in the study area during 2011–2016, A–L: spatial distribution (average values of different years), black dots indicate measurement points, M–O: comparison between sites inside and outside of the heated area in different seasons. For boxplot figures, the box border: the interquartile range (IQR); the horizontal line in the box: median value; the upper and lower vibrissae: 1.5 times IQR range beyond the upper and lower quartiles, respectively; grey dots: outliers. Significance indicated by the asterisks (unpaired Welch's *t*-test, *p-value*: *, <0.05; **, <0.01; ***, <0.001).

remain unchanged. Then, Welch's *t*-test and ANOSIM analysis were used to assess the difference in phytoplankton abundance and composition predicted by regression tree models between inside and outside heated areas.

All figures and analyses were developed with Surfer v11, Arcgis v10.3, Canoco 4.5 RStudio v4.1.2.

3. Result

3.1. Seasonal and spatial variation of environmental factors

Surface water temperature displayed a decreasing gradient from inshore to offshore in all seasons, with a temperature dropping by 1.1–3.6 °C within the 15 km from TNPP (Fig. 2 A–D). The temperature was highest in summer (28.10 ± 0.84 °C) and lowest in winter (5.36 ± 1.06 °C; Table 1). In contrast, salinity exhibited an increasing trend from inshore to offshore from winter to autumn (Fig. 2E–H). The highest salinity was observed in spring (30.62 ± 0.25) and the lowest in summer (28.19 ± 0.66; Table 1). Unlike temperature and salinity, the spatial distribution of TSM varies noticeably between seasons. Higher TSM was observed in the offshore area in winter, while higher values mainly occurred around TPNN in spring, summer, and autumn, closely corresponding with low-salinity and high-temperature environments (Fig. 2I–L). Lower TSM concentrations still appeared in summer (42.32 ± 23.41), while higher values mainly occurred in winter (60.61 ± 26.50 mg/L; Table 1). The temperature of sites inside of the heated area was significantly higher than sites outside the heated area in all the seasons except autumn ($t = 2.47$, $p < 0.05$ for winter; $t = 3.07$, $p < 0.01$ for spring; and $t = 3.99$, $p < 0.001$ for summer; Fig. 2M). Significant variance in salinity between these two regions was only observed in summer ($t = -3.21$, $p < 0.01$; Fig. 2N), indicating that the release of freshwater by the rivers only created a significant salinity gradient between both areas in summer. Unlike temperature and salinity, significant variance in TSM occurred in spring and summer ($t = 2.46$, $p < 0.05$ for spring; $t = 2.57$, $p < 0.05$ for summer; Fig. 2O).

The highest mean concentration of dissolved inorganic nitrogen (DIN) was observed in winter (25.49 ± 10.39 μmol/L), whereas the lowest mean value was observed in spring (13.83 ± 10.06 μmol/L, Table 1), with higher concentrations in the southeast sites during winter and in the sites around TNPP during summer (Fig. 3A–D). Unlike DIN, the average concentration of PO_4 was highest in autumn (0.86 ± 0.37 μmol/L) and lowest in spring (0.44 ± 0.32 μmol/L, Table 1). Less spatial variation of PO_4 concentration was observed during autumn and winter, while significant spatial variations were observed in spring and summer, with higher values around the river mouths (Fig. 3E–H). Mean $Si(OH)_4$ concentration was maximal in summer (13.17 ± 3.18 μmol/L) and minimal in spring (5.38 ± 2.55 μmol/L) (Table 1). The spatial distribution of $Si(OH)_4$ exhibited similar patterns to DIN, with the high-value areas appearing in the southeast area during winter and around TNPP during other seasons (Fig. 3I–L). Differences in nutrient concentrations between sites inside and outside the heated area were significant for DIN and PO_4 in summer ($t = 3.508$, $p < 0.001$ for DIN; $t = 3.3262$, $p < 0.01$ for PO_4; Fig. 3M and N) and for $Si(OH)_4$ in spring ($t = 3.201$, $p < 0.01$; Fig. 3O).

3.2. Seasonal and spatial variation of phytoplankton

3.2.1. Abundance

Phytoplankton abundance exhibited considerable seasonal and spatial variations (Fig. 4). It was highest in summer ($13.77 \times 10^6 \pm 17.51 \times 10^6$ cell/m^3) and lowest in winter ($4.14 \times 10^6 \pm 4.12 \times 10^6$ cell/m^3; Table 1). The spatial variation was more evident in spring and summer, with the highest values observed in the east side of the study area in spring and around TNPP in summer (Fig. 4B and C). In autumn and winter, spatial variation was less, and the high values mainly appeared in the south of the study area (site 11) and the south side of the water intake channel (site 2) (Fig. 4A, D). The *t*-test showed a significant difference in phytoplankton abundance between inside and outside sites in summer ($t = 4.563$, $p < 0.001$, Fig. 4E). However, no significant variance was observed between these two regions in other seasons, indicating that the impact of thermal stress on phytoplankton was more noticeable in summer than in other seasons.

3.2.2. Composition

We found 106 phytoplankton species, including 72 diatoms, 28 dinoflagellates, two cyanobacteria, and four other eukaryotic algae (cryptophyte, euglenophyte, chlorophyte, and chrysophyte) (Table S2).

Diatoms were the dominant phytoplankton in all sites and seasons, accounting for up to 99% of the phytoplankton community in both areas in winter and autumn and in the heated area in summer (Fig. 5A). In spring, the contribution of dinoflagellates to total abundance to 36.0% in the heated area, and 27.5% outside the heated area. The contribution of dinoflagellates in summer decreased, while the proportion of chrysophytes, euglenophytes, and cryptophytes increased. The contribution of diatoms was higher inside than outside the heated area, while the contributions of dinoflagellates and cryptophytes were lower inside than outside. The phytoplankton composition was only significantly different between the sites inside and outside the heated area in summer (ANOSIM: $R = 0.285$, $p = 0.001$, Fig. 5D).

To further understand the effect of thermal discharge on phytoplankton composition, we compared the seasonal variations in dominant species ($Y \geq 0.02$) between inside and outside the heated area (Fig. S1 and Fig. 6). The number of dominant species ranged from 10 to 19 across seasons during 2011–2016 with least dominant species appeared in

Table 1
Range and mean values (±SD) of environmental factors and phytoplankton abundance at different seasons in 2011–2016.

Parameters		Winter	Spring	Summer	Autumn
T (°C)	Range	3.56–10.39	15.71–23.76	25.92–32.59	10.01–18.43
	Mean ± SD	5.36 ± 1.45	19.01 ± 2.35	28.10 ± 1.34	14.61 ± 2.40
S	Range	27.53–31.89	29.10–32.42	25.59–31.18	26.93–31.24
	Mean ± SD	29.80 ± 0.99	30.62 ± 0.98	28.19 ± 1.31	29.22 ± 0.96
TSM (mg/L)	Range	28.60–139.50	1.43–212	4.18–121.50	9.00–119.8
	Mean ± SD	60.61 ± 26.50	44.18 ± 34.75	42.32 ± 23.41	58.30 ± 28.26
DIN (μmol/L)	Range	8.14–49.29	1.57–42.86	10.00–52.14	11.43–72.14
	Mean ± SD	25.49 ± 10.39	13.83 ± 10.06	23.32 ± 8.54	24.78 ± 8.31
PO_4 (μmol/L)	Range	0.16–2.68	0.03–1.21	0.26–1.48	0.39–1.97
	Mean ± SD	0.77 ± 0.38	0.44 ± 0.32	0.64 ± 0.25	0.86 ± 0.37
$Si(OH)_4$ (μmol/L)	Range	0.18–16.79	0.61–11.43	1.14–33.93	2.86–21.07
	Mean ± SD	7.83 ± 4.32	5.38 ± 2.55	13.17 ± 3.18	10.84 ± 4.52
PA ($\times 10^6$ cell/m^3)	Range	0.36–21.54	0.37–65.46	0.73–98.07	0.09–32.54
	Mean ± SD	4.14 ± 4.12	8.86 ± 11.15	13.77 ± 17.51	4.29 ± 5.92

T: temperature; *S*: salinity; TSM: total suspended matter; DIN: dissolved inorganic nitrogen, which is the sum of NO_3, NO_2, and NH_4; PO_4: dissolved inorganic phosphate; $Si(OH)_4$: dissolved silicate; PA: phytoplankton abundance.

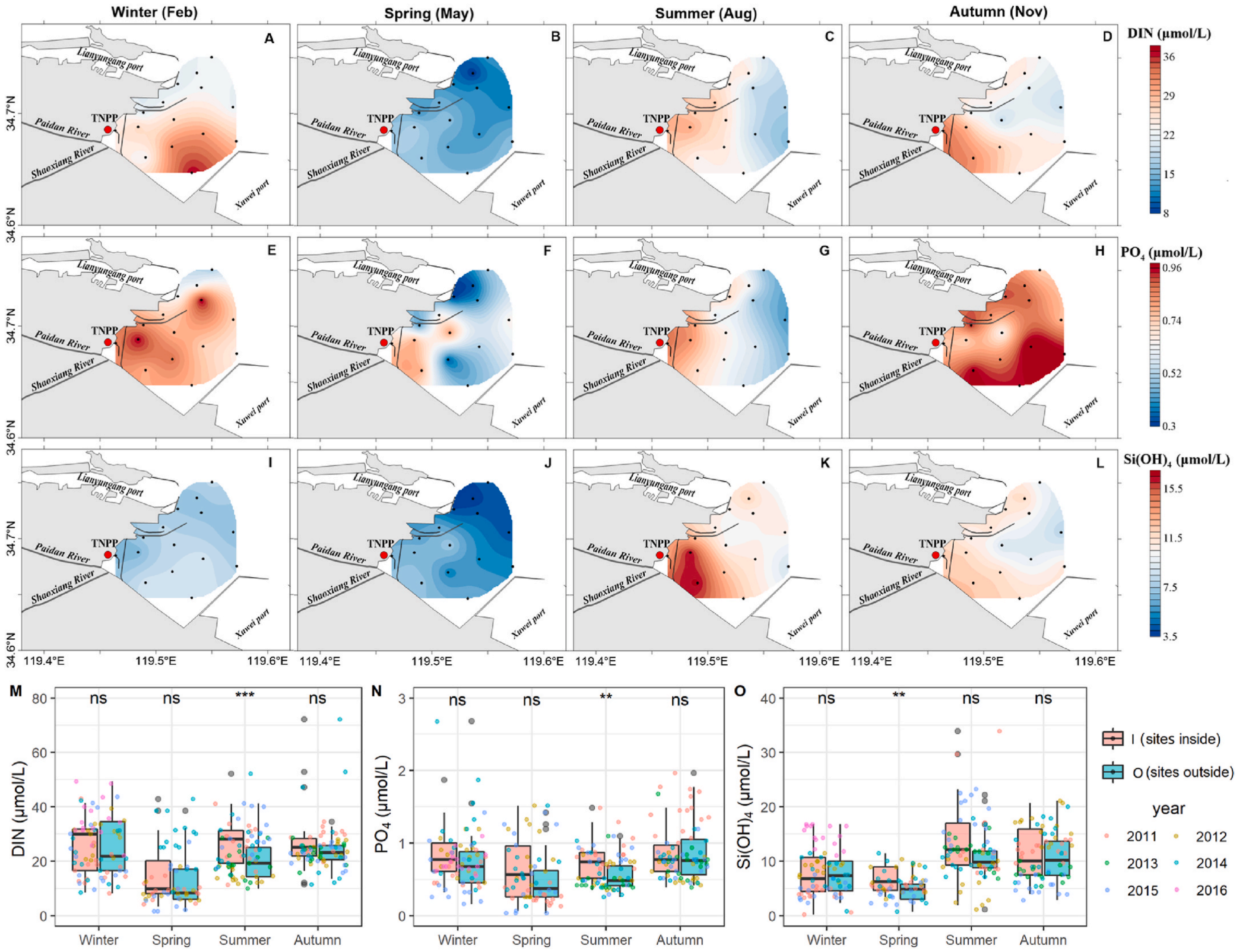

Fig. 3. Spatial and temporal variation of DIN, PO_4, and $Si(OH)_4$ in the study area during 2011–2016, A–L: spatial distribution (average values of different years), black dots indicate measurement points, M–O: comparison between sites inside and outside of the heated area in different seasons. For the detailed introduction of boxplot figures, please see the caption of Fig. 2.

summer (Fig. S1). The most dominant species are diatoms, followed by dinoflagellate and euglenophyte (Fig. S1). Among the dominant species, *Skeletonema costatum* sensu lato was the most abundant species overall. While *S. costatum* followed relatively similar trends inside and outside the heated area, and their contribution inside was higher than outside in all the seasons (Fig. 6A). Other dominant species included *Pseudo-nitzschia, Prorocentrum minimum, Chaetoceros densus Chaetoceros* sp. and *Chaetoceros curvisetus, and their abundance* varied across years and study areas (Fig. 6A). Differences in species dominance between sites inside and outside the heated area were only significant in summer (ANOSIM: $R = 0.241$, $p = 0.001$, Fig. 6D).

3.3. *Relationship between environmental factors and phytoplankton community*

A redundancy analysis (RDA) was used to investigate relationships between the main dominant species (blue lines in Fig. 7) and environmental variables (red lines in Fig. 7) in different seasons.

In winter, the first two axes explained 6.5% and 2.4% of the variation, respectively (Fig. 7A). The first axis was mainly formed by PO_4 concentration, while the second axis was influenced primarily by temperature and TSM concentrations. Most dominant species were associated with a high PO_4 concentration environment. While *P. pungens* was associated with relatively high TSM and low-temperature environment (Fig. 7A). In spring, the first two axes of the RDA explained approximately 59.0% and 1.1% of the variation (Fig. 7B). The first axis was mainly contributed by PO_4 and $Si(OH)_4$, while the second was primarily contributed by salinity and temperature. *Skeletonema costatum* sensu lato and *P. minimum*, which were the dominant phytoplankton species in spring cruises, were positively correlated with high PO_4 and $Si(OH)_4$ concentrations (Fig. 7B). In contrast, *C. densus* with high dominance in 2014 was associated with low temperature and high DIN (Fig. 7B). In summer, the first axis of the RDA, which accounted for 59.8% of the total variation, was mainly contributed by temperature (Fig. 7C). The main dominant species (*S. costatum*) was positively associated with high temperature, while *Chaetoceros* sp. and *C. curvisetus* were correlated with high nutrient levels (Fig. 7C). In autumn, the first two axes of the RDA explained 15.8% and 8.8% of the variation (Fig. 7D). The first axis was mainly contributed by temperature and inversely by $Si(OH)_4$, whereas the second axis was by TSM concentration. The relationship between environmental variables and dominant species can be divided into three categories. The major dominant species (*S. costatum*) was associated with high nutrient levels and low salinity (Fig. 7D). *Chaetoceros catracanei*, *Chaetoceros* sp., *Eucampia zodiacus*, and *Thalassiosira* sp. were moderately associated with high-temperature environments (Fig. 7D). The other dominant species were related to high TSM concentration

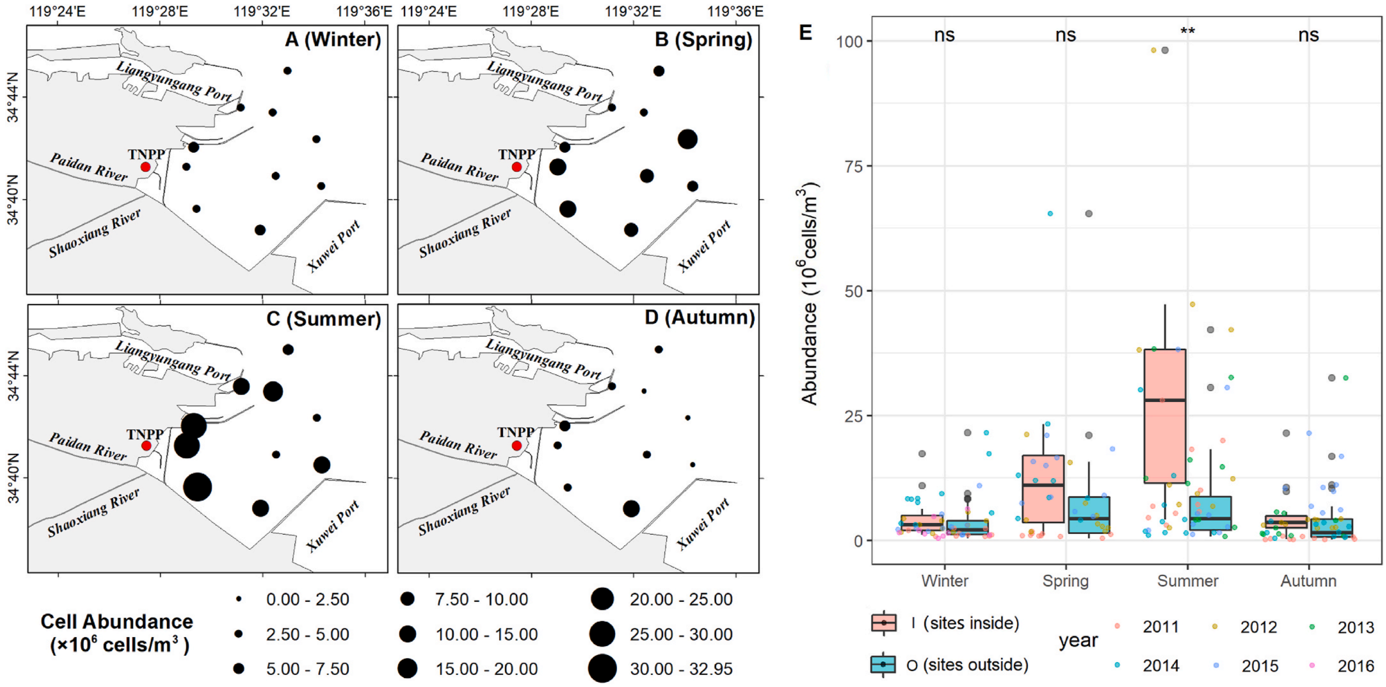

Fig. 4. Spatial and temporal variation of phytoplankton abundance in the study area during 2011–2016, A–D: spatial distribution (average values of different years), black dots indicate measurement points, E: comparison between sites inside and outside of the heated area in different seasons. For the detailed introduction of boxplot figures, please see the caption of Fig. 2.

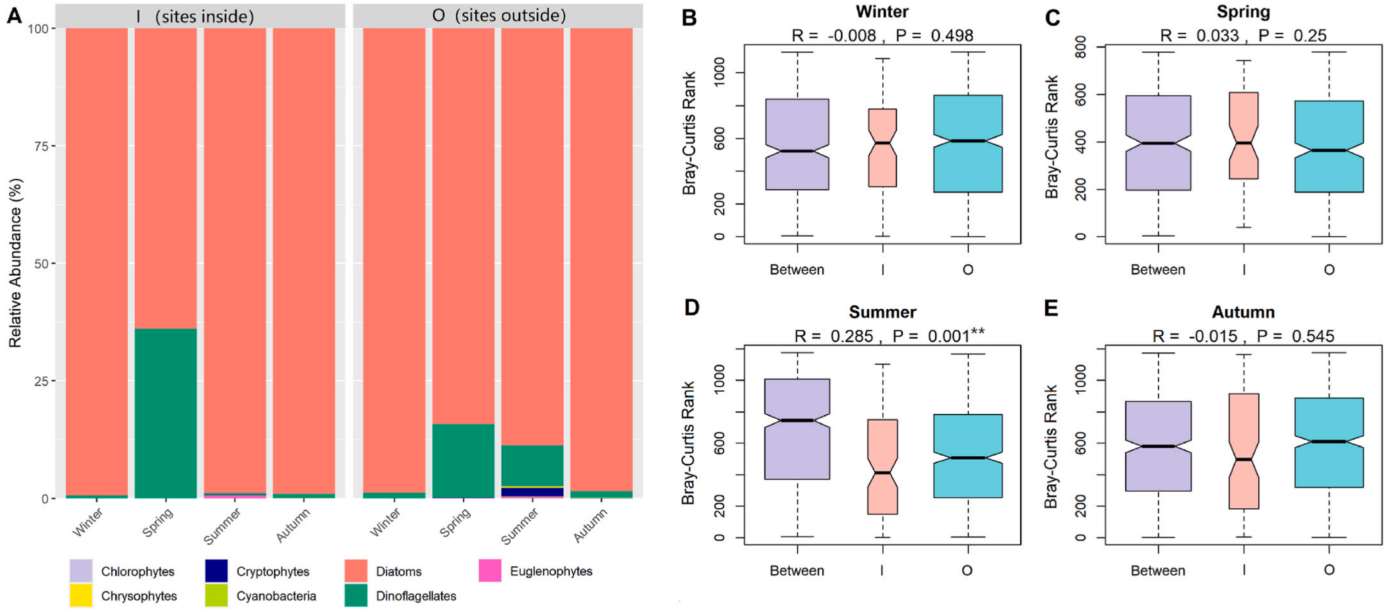

Fig. 5. Comparison of phytoplankton composition between sites inside (I) and outside (O) of the heated area in different seasons, A: relative abundance of different phytoplankton in different seasons (average data of different years), B–E: analysis of similarities (ANOSIM). For ANOSIM figures, the Y-axis: the dissimilarity rank distribution; the box border: the interquartile range (IQR); the horizontal line in the box: median value; the upper and lower vibrissae: the 1.5 times IQR range beyond the upper and lower quartiles; between reflects the differences between groups, and groups I and O represent the differences within groups. The test statistic R is constrained between the values −1 to 1, where R > 0 suggests more similarity within groups and R < 0 suggests more similarity between groups than within groups. P indicates significance (*, <0.05; **, <0.01; ***, <0.001).

environments (Fig. 7D).

3.4. *Effect of thermal discharge on phytoplankton variation in summer*

The regression tree analysis was used to assess the relative importance of thermal discharge and environment variation in determining the significant difference in phytoplankton abundance and dominant species in summer. The results showed that temperature was the most important driver for the distributions of phytoplankton abundance and the main dominant species (*S. costatum*) (Figs. S2A and C). The other two common dominant species, which have a higher proportion of phytoplankton abundance in outside sites, were mainly affected by silicate

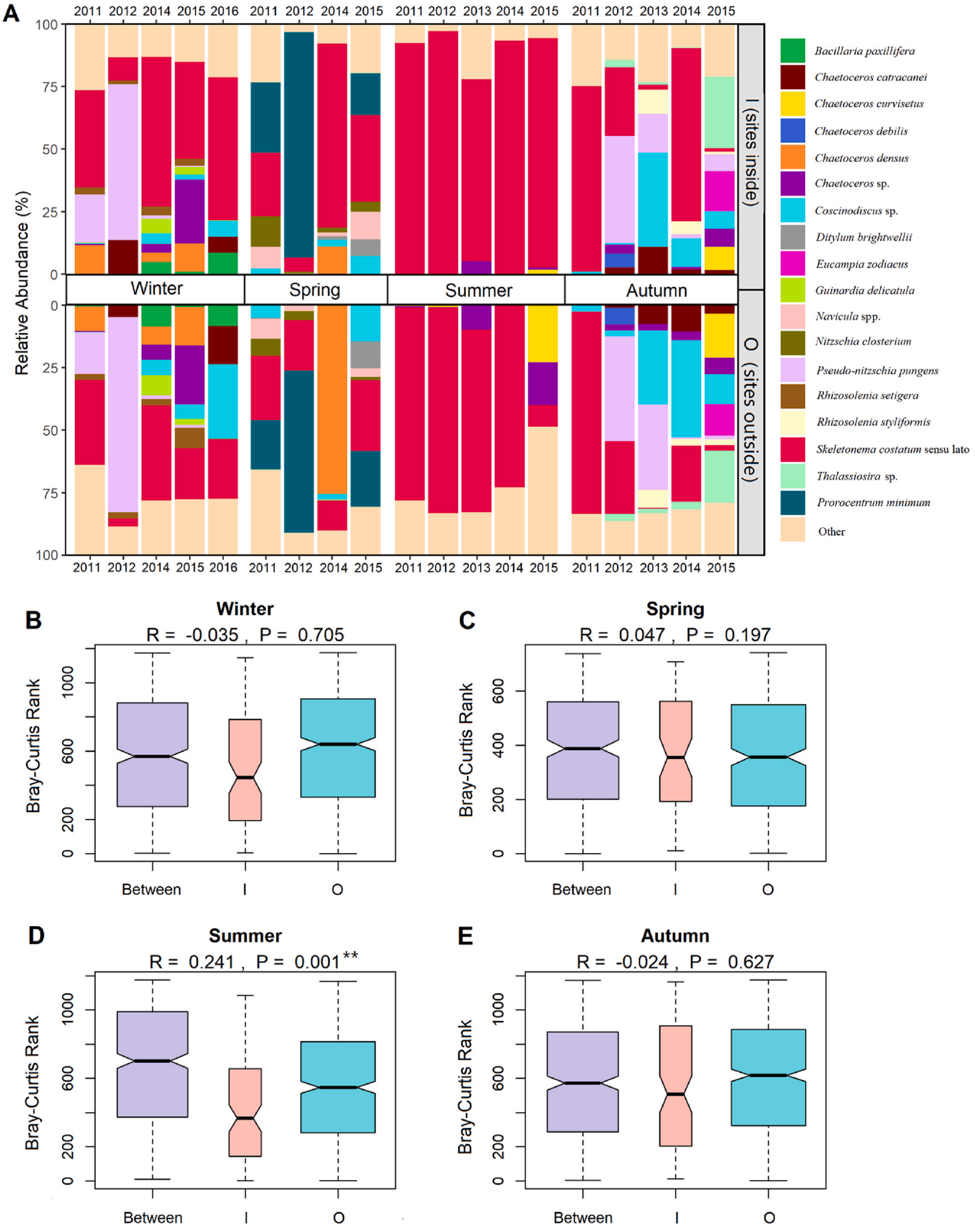

Fig. 6. Comparison of dominant species between sites inside (I) and outside (O) of the heated area in different seasons, A: relative abundance of dominant species (only the dominant species with mean dominance during 2011–2016 not less than 0.02 ($Y \geq 0.02$) were selected to display more clearly), B–E: ANOSIM analysis. For the detailed introduction of ANOSIM figures, please see the caption of Fig. 5.

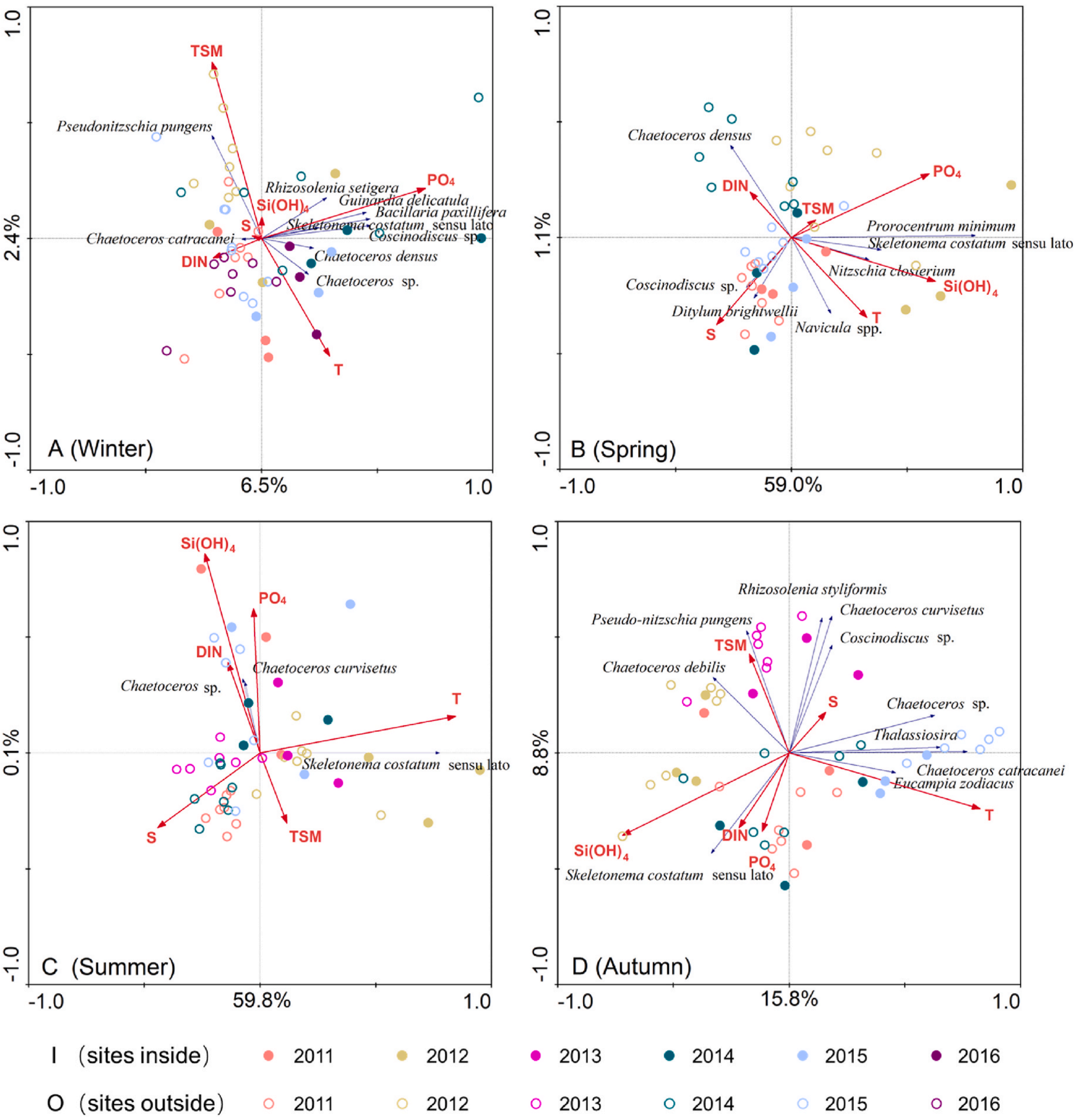

Fig. 7. Redundancy analysis (RDA) correlation triplots of the main dominant species (blue line) in relation to environmental variables (red line) in different seasons. Circular symbols illustrate where samples originated from (solid circles: sites inside of the heated area, hollow circles: sites outside of the heated area, color: sampling year). (For interpretation of the references to color in this figure legend, the reader is referred to the Web version of this article.)

and TSM (Figs. S2B and D).

To discriminate the effect of thermal stress caused by the NPP from other variables, we used regression tree models to predict the phytoplankton abundance and species dominance in summer, assuming the water temperature in both study areas was the same (= mean summer temperature outside the heated area of each cruise). The model predicted that the phytoplankton abundances in the inside sites were lower than observed and were no longer significantly different from the sites outside the heated area ($t = 1.98$, $p > 0.05$; Fig. 8A). Further statistical analysis based on predicted dominated species showed that significant difference in phytoplankton composition between sites inside and outside the heated area in summer would disappear if the water temperature in both regions were the same (ANOSIM: $R = 0.079$, $p > 0.05$; Fig. 8B).

4. Discussion

4.1. Effect of thermal discharge on the environmental factors

Substantial evidence supports that thermal effluents from NPPs can increase the temperature of the receiving waters in temperate areas (Rajagopal et al., 2012). In this study, we also found a marked increase in water temperature within a range of 10–15 km around TNPP (Fig. 2A–D), and the high-value area corresponded well with the heated area previously reported (Nie et al., 2021; Wang and Xiong, 2013). Consistent with previous studies, temperature change outside this range was low (<1 °C), reflecting temperature dissipation as TNPP effluents away from the source (Jia et al., 2016; Zhang et al., 2019). This indicates that the scale and extent of thermal effect are limited to 10–15 km off TNPP.

Furthermore, previous studies reported that the increase in temperature caused by thermal discharge not only increases temperature but

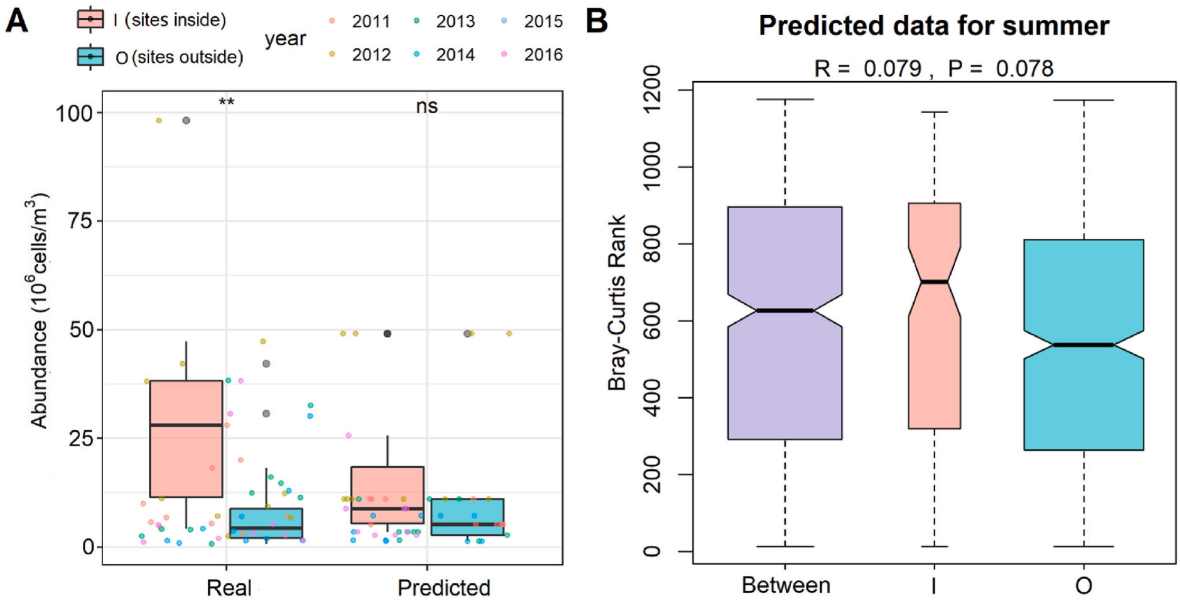

Fig. 8. Comparison of phytoplankton abundance and composition predicted by regression tree model between sites inside (I) and outside(O) of the heated area in summer, A: unpaired Welch's *t*-test of real and predicted phytoplankton abundance (significance indicated by the asterisks *p*-value: *, <0.05; **, <0.01; ***, <0.001); B: ANOSIM analysis based on predicted dominant species. For the detailed introduction of ANOSIM figure, please see the caption of Fig. 5.

also can elevate the concentration of dissolved nutrients by promoting the conversion of nutrients attached to suspended solids to soluble forms (Poornima et al., 2012) and the release rate of phosphorus increases dramatically as temperatures rise above 15 °C (Karr and Schlosser, 1978). During 2011–2016, the affected area of thermal discharge was stable, with the heated area ranging from 21.09 to 24.05 km^2 (Nie et al., 2021). However, higher annual and seasonal variations and less spatial variations in nutrient concentrations were observed during 2011–2016 (Fig. 3M, N, O). RDA analysis showed that nutrients and temperature were uncorrelated in most seasons, indicating that nutrient concentrations might be affected by other factors rather than thermal discharge. The significant difference in DIN and PO_4 between sites inside and outside of the heated area was only observed in summer with high freshwater input and low salinity, and high DIN and PO_4 values were mainly consistent with low salinity area, indicating high DIN and PO_4 concentrations probably originated from the two rivers around TNPP during the period. RDA analysis showed that nutrients were significantly negatively correlated with salinity but nearly uncorrelated with temperature in summer (Fig. 7C), confirming that the freshwater input rather than thermal discharge was the main reason for the spatial differences in nutrient concentrations during the period. In winter, the seawater is well-mixed in the Yellow Sea, driven by strong northeast winds, and the water column is vertically homogeneous (Zhang et al., 2008). Nutrient distribution did not have a defined variation pattern during winter, and the accumulated nutrients at the bottom brought up by strongly vertical mixing may be the main source of nutrients (Fu et al., 2009). These results indicate that the effects of thermal discharge on nutrient concentration were much less than that on temperature in temperate regions.

4.2. Effects of thermal discharge on phytoplankton abundance

Water temperature is a key environmental driver of phytoplankton abundance in aquatic ecosystems (Boyce et al., 2010). Previous studies suggested that the increase in temperature caused by thermal effluents from NPPs has the potential to cause thermal stress on phytoplankton and other aquatic organisms (Begun and Maslennikov, 2021; Poornima et al., 2012). However, studies performed in different regions, seasons, and years have shown diverse effects of thermal discharge on phytoplankton abundance. The increase in temperature caused by thermal discharge might stimulate, inhibit, or not affect the growth of the phytoplankton community (Jia et al., 2016; Krishnakumar et al., 1991; Lin et al., 2018; Morgan and Stross, 1969).

Our study across five years found that the differences in phytoplankton abundance between sites inside and outside of the heated area were only significantly different in summer, with temperatures ranging from 25.92 to 32.59 (Fig. 4E), indicating that the thermal effect on phytoplankton community is more evident in warm seasons. Furthermore, the regression tree analysis showed that temperature is the most important factor driving phytoplankton abundance during summer and that the model predicts that the phytoplankton abundance in the inside sites is the same as in the outside sites if water temperature is the same (Fig. S2A). This confirms that the temperature increase in the water caused by TNPP effluents is the main driver of the changes in phytoplankton community around NPP located in temperate regions. Our results further support previous findings that the impact of thermal effluents of NPP on phytoplankton community varies between seasons (Jia et al., 2016; Krishnakumar et al., 1991; Lin et al., 2018). In addition to a higher temperature, significantly higher DIN and PO_4 concentrations were also observed in the inside sites during summer (Fig. 3), indicating that high nutrient concentrations may synergistically promote phytoplankton growth. This finding well explains previous results that the frequency and duration of algal blooms in subtropical eutrophic waters are often highly associated with thermal discharge from power plants (Jiang et al., 2019a; Jiang et al., 2019b; Yu et al., 2007). Thermal discharge has no significant effect on phytoplankton from autumn to spring (cold season) partly explains why no apparent effect of thermal discharge from NPPs on phytoplankton was detected in low seawater temperature areas (Ilus et al., 1987; Keskeital and Ilus, 1987; Lo et al., 2004).

Seasonal differences in the effect of thermal discharge on phytoplankton abundance in temperate regions may also be related to the different hydrodynamic environments between seasons. During winter, the shorter daytime and the vertical mixing in temperate areas make it difficult for phytoplankton to remain on surface water to obtain enough light (Liu et al., 2015; Mahadevan et al., 2012), thus reducing the positive effect of temperature on phytoplankton growth during the cold season. However, the large supply of nutrients by river inputs during summer (wet seasons), coupled with appropriate growth temperatures of dominant Diatom (Muhammad-Adlan et al., 2012; Patrick, 1971; Poornima et al., 2005), enhance the effect of temperature rise on phytoplankton growth. The finding explains why the effect of thermal discharge on phytoplankton is more pronounced in reservoirs and inner bays where the hydrodynamic dynamics are more stable (Jia et al., 2016; Jiang et al., 2019b; Xu et al., 2021), suggesting that the effects of thermal discharge from NPPs on phytoplankton might also be influenced by hydrodynamic forces (Karr and Schlosser, 1978; Rajagopal et al., 2012; Wang and Xiong, 2013).

Our results suggest that thermal effects from NPPs on phytoplankton abundance in temperate regions are seasonal and short, depending on site-specific nutrient concentrations and ambient water temperature. The positive effect of temperature on phytoplankton abundance is more evident in summer with high nutrient concentration, warm water temperature, and stable hydrodynamic conditions.

4.3. Effect of thermal discharge on phytoplankton community

Optimal growth temperature varies with species (Grimaud et al., 2015; Pane et al., 2001; Richardson et al., 2008), and thus phytoplankton composition and the succession of dominant species are often driven by temperature (Lewandowska and Sommer, 2010; Liu et al., 2017). However, there has been no consensus on the effect of thermal discharge on phytoplankton composition in temperate areas. Results from different years show that thermal discharge might stimulate, inhibit, or not significantly affect the growth of phytoplankton (Chuang et al., 2009; Li et al., 2011; Ilus et al., 1987; Keskeital and Ilus, 1987; Lo et al., 2004), and the impact intensity varies notably in different seasons (Jia et al., 2016; Krishnakumar et al., 1991; Lin et al., 2018). Our results showed that the inter-annual variation in temperature and dominant species were more evident than the spatial variation, especially during autumn (Figs. 2 and 6, and Fig. S1). RDA analysis confirmed the low similarity of phytoplankton community between years in autumn (Fig. 7D). In addition, different phytoplankton species responded differently to environmental variables, suggesting that the temperature-driven variation of phytoplankton community may affect the identification of the effect of the thermal discharges based on the statistical analyses of RDA, especially in those seasons with significant temperature variation. The finding partly explains why previous studies of the effects of thermal emissions on phytoplankton communities varied markedly.

In this study, phytoplankton composition only differed between sites inside and outside the heated area in summer (Fig. 6D), suggesting that thermal discharge cannot cause a significant variation in phytoplankton composition in most seasons except summer. However, phytoplankton composition is not only affected by water temperature but by several other environmental variables (e.g., salinity, nutrient conditions, and light) (Amorim et al., 2020; David et al., 2020; Yang et al., 2020). Therefore, it is challenging to identify the relative importance of thermal discharge and environmental variation on the significant difference in phytoplankton community between inside and outside sites in summer because of the significant spatial and inter-annual variations of environmental factors (Field et al., 1998). We used regression tree models confirming that phytoplankton composition between inside and outside sites in summer would disappear when temperature differences caused by thermal discharge were removed, indicating that thermal discharge is the main reason for the significant difference in phytoplankton composition between inside sites and outside sites.

During summer, the significant difference in phytoplankton composition between sites inside and outside of the heated area was mainly reflected in the higher proportion of diatoms, and lower proportion of dinoflagellate and cryptophytes in the heated area (Fig. 5A), consistent with previous findings around other NPPs (Jia et al., 2016; Lin et al., 2018; Xu et al., 2021). Additionally, the relative abundance of dinoflagellates around TNPP was lower than in other regions of Haizhou Bay in summer (Li et al., 2017; Zhang et al., 2021; Zhu et al., 2017), indicating that elevated temperature caused by NPPs effluents may increase diatom and decreases the other phylum (Kim and Seo, 2018; Xu et al., 2021). A wide tolerable range of water temperature (Patrick, 1971), less susceptibility to mechanical damage due to the siliceous shells (Poornima et al., 2006), and high concentrations of $Si(OH)_4$ around TNPP may be the main reasons for higher abundance of diatoms in inside sites in summer.

Different phytoplankton populations grow at different rates under fluctuating temperature conditions, and the species that can quickly adapt to fluctuating environments have a higher abundance (Grimaud et al., 2015; Pane et al., 2001; Richardson et al., 2008). In our study, *S. costatum* was the most reoccurring dominant species with high dominance in all seasons. Their contribution in sites inside the heated area was always higher than that outside (Fig. 6A), indicating that *S. costatum* is better adapted to thermal stress. This may be attributed to the fact that the euryhaline and eurythermal characteristics of the species make it able to better adapt to the highly fluctuating seawater temperature and salinity around TNPP (Liu et al., 2020; Zhao et al., 2018). The contribution of *S. costatum* increased significantly in summer, especially in the inside sites, which was as high as 91.26% (Fig. 6A). The results of RDA analysis showed that *S. costatum* was highly positively associated with temperature during the period (Fig. 7C), supporting evidence that thermal discharge plays an important role in the high abundance of this species.

In general, the findings of this study provide evidence that the effect of thermal discharge on phytoplankton community structure is dynamic and vary with seasons (Chuang et al., 2009; Li et al., 2011; Lin et al., 2018; Poornima et al., 2005), and that the effect is more notable in warm seasons than in cold seasons. In addition, thermal discharge from TNPP may significantly decrease the abundance of vulnerable species and increase the abundance of species with stronger heat resistance in summer, thus reshaping phytoplankton composition.

5. Conclusion

In this study, a 5-year continuous monitoring program was performed to evaluate the effect of thermal discharge from TNPP on the seasonal distribution of phytoplankton communities in the temperate coastal area. Our results suggest that the thermal effects from NPPs on phytoplankton communities in the temperate area are seasonal, depending on site-specific nutrient circumstances and the ambient seawater temperature. In winter, spring, and autumn, when the average temperature is below 20 °C, the thermal discharge from TNPPs cannot cause significant changes in phytoplankton abundance and community structure. However, the thermal discharge can significantly promote the population growth of phytoplankton and reshape phytoplankton composition around TNPP in summer with high ambient temperature, abundant nutrients, and stable hydrodynamic conditions. During summer, *S. costatum*, which can adapt quickly under fluctuating environments with stronger heat resistance, has a significantly higher abundance around TNPP, thus significantly increasing the contribution of diatoms in the heated area. Additionally, we confirmed for the first time that the difference between inside and outside sites in summer was caused by temperature increases rather than the variation of other environmental factors. Overall, the findings of this study improve our understanding of the ecological effect of thermal discharge from NPPs in temperate areas.

Credit author statement

Jingjing Zhang: conceived the ideas and wrote the manuscript; **Yibin Wang:** collected and analyzed the samples and edited the manuscript; **Daniel Ottmann:** edited the manuscript and plotted the figures. **Peng Cao:** analyzed the environmental factor; **Jisong Yang, Junbao Yu, and Zhenbo Lv:** supervision and funding acquisition. All

authors contributed critically to the drafts and gave final approval for publication.

Declaration of competing interest

The authors declare that they have no known competing financial interests or personal relationships that could have appeared to influence the work reported in this paper.

Data availability

The authors do not have permission to share data.

Acknowledgments

This work was sponsored by Natural Science Foundation of Shandong Province (Grant Nos. ZR2022MD009 and ZR2022MD079), and National Natural Science Foundation of China (Grant Nos. U1806218 and U2006215).

Appendix A. Supplementary data

Supplementary data to this article can be found online at https://doi.org/10.1016/j.envpol.2022.120898.

References

Amorim, C.A., Dantas, E.W., Moura, A.D.N., 2020. Modeling cyanobacterial blooms in tropical reservoirs: the role of physicochemical variables and trophic interactions. Sci. Total Environ. 744, 140659 https://doi.org/10.1016/j.scitotenv.2020.140659.

Bamber, R.N., Seaby, R.M., 2004. The effects of power station entrainment passage on three species of marine planktonic crustacean, Acartia tonsa (Copepoda), Crangon crangon (Decapoda) and Homarus gammarus (Decapoda). Mar. Environ. Res. 57 (4), 281–294. https://doi.org/10.1016/j.marenvres.2003.08.002.

Begun, A.A., Maslennikov, S.I., 2021. Influence of the technical ecosystem of the electric power plant (vladivostok) on the phytoplankton of the Japanese sea. Water Resour. 48 (3), 404–412. https://doi.org/10.1134/s0097807821030052.

Behrenfeld, M.J., Boss, E.S., 2014. Resurrecting the ecological underpinnings of ocean plankton blooms. Ann. Rev. Mar. Sci 6, 167–194. https://doi.org/10.1146/annurev-marine-052913-021325.

Boyce, D.G., Lewis, M.R., Worm, B., 2010. Global phytoplankton decline over the past century. Nature 466 (7306), 591–596. https://doi.org/10.1038/nature09268.

Choi, D.H., Park, J.S., Hwang, C.Y., Huh, S.H., Cho, B.C., 2002. Effects of thermal effluents from a power station on bacteria and heterotrophic nanoflagellates in coastal waters. Mar. Ecol. Prog. Ser. 229, 1–10. https://doi.org/10.3354/meps229001.

Chuang, Y.L., Yang, H.H., Lin, H.J., 2009. Effects of a thermal discharge from a nuclear power plant on phytoplankton and periphyton in subtropical coastal waters. J. Sea Res. 61 (4), 197–205. https://doi.org/10.1016/j.seares.2009.01.001.

David, V., Tortajada, S., Savoye, N., Breret, M., Lachaussee, N., Philippine, O., Robin, F. X., Dupuy, C., 2020. Impact of human activities on the spatio-seasonal dynamics of plankton diversity in drained marshes and consequences on eutrophication. Water Res. 170, 115287 https://doi.org/10.1016/j.watres.2019.115287.

Fu, M.Z., Wang, Z.L., Li, Y., Li, R.X., Sun, P., Wei, X.H., et al., 2009. Phytoplankton biomass size structure and its regulation in the Southern Yellow Sea (China): seasonal variability. Continent. Shelf Res. 29 (18), 2178–2194. https://doi.org/10.1016/j.csr.2009.08.010.

Field, C.B., Behrenfeld, M.J., Randerson, J.T., Falkowski, P., 1998. Primary production of the biosphere: integrating terrestrial and oceanic components. Science 281 (5374), 237–240. https://doi.org/10.1126/science.281.5374.237.

Gómez, M.I., Piola, A.R., Kattner, G., Alder, V.A., 2011. Biomass of autotrophic dinoflagellates under weak vertical stratification and contrasting chlorophyll levels in subantarctic shelf waters. J. Plankton Res. 33 (8), 1304–1310. https://doi.org/10.1093/plankt/fbr031.

Grimaud, G.M., Le Guennec, V., Ayata, S.-D., Mairet, F., Sciandra, A., Bernard, O., 2015. Modelling the effect of temperature on phytoplankton growth across the global ocean. IFAC-PapersOnLine 48 (1), 228–233. https://doi.org/10.1016/j.ifacol.2015.05.059.

Hu, J.H., 2004. The coastal currents offshore the nuclear power plants at northern taiwan. J. Mar. Sci. Technol. 12 (5), 355–363. https://doi.org/10.51400/2709-6998.2256.

Hu, L., Shi, X., Guo, Z., Wang, H., Yang, Z., 2013. Sources, dispersal and preservation of sedimentary organic matter in the Yellow Sea: the importance of depositional hydrodynamic forcing. Mar. Geol. 335, 52–63. https://doi.org/10.1016/j.margeo.2012.10.008.

Huang, W., Wang, W., Zhang, W., Zhang, J., 2012. Analysis of characteristics of the tides and the tidal currents in adjacent waters of Lianyungang port. Zhe. Hydrotech. 3, 1–5. https://doi.org/10.3969/j.issn.1008-701X.2012.03.001 (In Chinese).

Ikäheimonen, T., Klemola, S., Ilus, E., Sjoeblom, K.-L., 1995. Monitoring of Radionuclides in the Vicinities of Finnish Nuclear Power Plants in 1991-1992. Report STUK-A-121. Finnish Centre for Radiation and Nuclear Safety, Helsinki, pp. 1–96, 1995.

Ilus, E., Sjöblom, K., Aaltonen, H., Klemola, S., Arvela, H., 1987. Monitoring of Radioactivity in the Environs of Finnish Nuclear Power Stations in 1986. Finnish Centre for Radiation and Nuclear Safety.

Jia, H.L., Zheng, S., Xie, J., Ying, X.M., Zhang, C.P., 2016. Influence of geographic setting on thermal discharge from coastal power plants. Mar. Pollut. Bull. 111 (1–2), 106–114. https://doi.org/10.1016/j.marpolbul.2016.07.024.

Jiang, Z., Du, P., Liu, J., Chen, Y., Zhu, Y., Shou, L., Zeng, J., Chen, J., 2019a. Phytoplankton biomass and size structure in Xiangshan Bay, China: current state and historical comparison under accelerated eutrophication and warming. Mar. Pollut. Bull. 142, 119–128. https://doi.org/10.1016/j.marpolbul.2019.03.013.

Jiang, Z., Gao, Y., Chen, Y., Du, P., Zhu, X., Liao, Y., Liu, X., Zeng, J., 2019b. Spatial heterogeneity of phytoplankton community shaped by a combination of anthropogenic and natural forcings in a long narrow bay in the East China Sea. Estuar. Coast Shelf Sci. 217, 250–261. https://doi.org/10.1016/j.ecss.2018.11.028.

Karr, J.R., Schlosser, I.J., 1978. Water resources and the land-water interface. Science 201 (4352), 229–234. https://doi.org/10.1126/science.201.4352.229.

Keskeital, J., Ilus, E., 1987. Aquatic Macrophytes outside the Olkiluoto Nuclear Power Station, West Coast of Finland. Annales Botanici Fennici. JSTOR, pp. 1–21.

Khan, S.U.D., Nakhabov, A.V., 2020. Nuclear Reactor Technology Development and Utilization. Elsevier Woodhead Publishing, London, pp. 1–4.

Kim, D.G., Seo, I.W., 2018. Numerical modeling of the tee thermal diffuser in coastal regions. Coast Eng. J. 43 (1), 59–78. https://doi.org/10.1142/s057856340100027x.

Krishnakumar, V., Sastry, J., Swamy, G.N., 1991. Implication of thermal discharges into the sea-a review. Indian J. Environ. Protect. 11, 525–527.

Langford, T., 1990. Ecological Effects of Thermal Discharges. Elsevier Applied Science Publishers, London, pp. 28–103.

Lee, P.W., Tseng, L.C., Hwang, J.S., 2018. Comparison of mesozooplankton mortality impacted by the cooling systems of two nuclear power plants at the northern Taiwan coast, southern East China Sea. Mar. Pollut. Bull. 136, 114–124. https://doi.org/10.1016/j.marpolbul.2018.09.003.

Lewandowska, A., Sommer, U., 2010. Climate change and the spring bloom: a mesocosm study on the influence of light and temperature on phytoplankton and mesozooplankton. Mar. Ecol. Prog. Ser. 405, 101–111. https://doi.org/10.3354/meps08520.

Li, D.P., Zhang, S., Shi, Y.Q., Zhang, Y., Huang, H., 2017. Different seasonal changes of phytoplankton community in the marine farming of Haizhou bay. Ecol. Environ. Sci. 26 (2), 285–295. https://doi.org/10.16258/j.cnki.1674-5906.2017.02.014 (In Chinese).

Li, T., Liu, S., Huang, L., Huang, H., Lian, J., Yan, Y., Lin, S., 2011. Diatom to dinoflagellate shift in the summer phytoplankton community in a bay impacted by nuclear power plant thermal effluent. Mar. Ecol. Prog. Ser. 424, 75–85. https://doi.org/10.3354/meps08974.

Lin, J., Zou, X.Q., Huang, F.M., 2018. Effects of the thermal discharge from an offshore power plant on plankton and macrobenthic communities in subtropical China. Mar. Pollut. Bull. 131, 106–114. https://doi.org/10.1016/j.marpolbul.2018.04.005.

Liu, C.Y., Xu, G.B., Deng, X., Zhang, H.H., Liu, T., Yang, G.P., 2020. Changes in concentrations of biogenic sulfur compounds in coastal waters off Qingdao, China during an Ulva prolifera bloom. Mar. Pollut. Bull. 152 https://doi.org/10.1016/j.marpolbul.2020.110940.

Liu, C., Sun, Q.W., Xing, Q.G., Wang, S.F., Tang, D.L., Zhu, D.H., Xing, X., 2019. Variability in phytoplankton biomass and effects of sea surface temperature based on satellite data from the Yellow Sea, China. PLoS One 14 (8), e0220058. https://doi.org/10.1371/journal.pone.0220058.

Liu, H., Weibel, J., Groll, E., 2017. Performance analysis of an updraft tower system for dry cooling in large-scale power plants. Energies 10 (11), 1812. https://doi.org/10.3390/en10111812.

Liu, X., Chiang, K.P., Liu, S.M., Wei, H., Zhao, Y., Huang, B.Q., 2015. Influence of the Yellow Sea warm current on phytoplankton community in the central Yellow Sea. Deep-Sea Res. Part I 106, 17–29. https://doi.org/10.1016/j.dsr.2015.09.008.

Lo, W.T., Hwang, J.J., Hsu, P.K., Hsieh, H.Y., Tu, Y.Y., Fang, T.H., Hwang, J.S., 2004. Seasonal and spatial distribution of phytoplankton in the waters off nuclear power plants, north of Taiwan. J. Mar. Sci. Technol. 12 (5), 372–379. https://doi.org/10.51400/2709-6998.2258.

Lofton, M.E., Leach, T.H., Beisner, B.E., Carey, C.C., 2020. Relative importance of top-down vs. bottom-up control of lake phytoplankton vertical distributions varies among fluorescence-based spectral groups. Limnol. Oceanogr. 65 (10), 2485–2501. https://doi.org/10.1002/lno.11465.

Ma, Z., Gao, K., Li, W., Xu, Z., Lin, H., Zheng, Y., 2011. Impacts of chlorination and heat shocks on growth, pigments and photosynthesis of Phaeodactylum tricornutum (Bacillariophyceae). J. Exp. Mar. Biol. Ecol. 397 (2), 214–219. https://doi.org/10.1016/j.jembe.2010.12.009.

Mahadevan, A., D'Asaro, E., Lee, C., Perry, M.J., 2012. Eddy-driven stratification Initiates North Atlantic spring phytoplankton blooms. Science 337 (6090), 54–58. https://doi.org/10.1126/science.1218740.

Mask, A.C., O'Brien, J.J., Preller, R., 1998. Wind-driven effects on the Yellow Sea warm current. J. Geophys. Res. 103, 30713–30729. https://doi.org/10.1029/1998JC900007.

Mercado, L.M., Gomez, N., 1999. Effects of a nuclear power plant on phytoplankton structure of the lower Paraná River. Interciencia 24 (1), 36–41.

Morgan, R.P., Stross, R.G., 1969. Destruction of phytoplankton in the cooling water supply of a steam slectric station. Chesap. Sci. 10 (3/4), 165–171. https://doi.org/10.2307/1350453.

Muhammad-Adlan, A., Wan-Maznah, W., Khairun, Y., Chuah, C., Shahril, M., Noh, M., 2012. Tropical marine phytoplankton assemblages and water quality characteristics associated with thermal discharge from a coastal power station. J. Nat. Sci. Res. 2, 88–100. https://doi.org/10.1016/0025-326x(80)90410-5.

Nie, P., Wu, H., Xu, J., Wei, L., Zhu, H., Ni, L., 2021. Thermal pollution monitoring of tianwan nuclear power plant for the past 20 Years based on landsat remote sensed data. IEEE J. Sel. Top. Appl. Earth Obs. Rem. Sens. 14, 6146–6155. https://doi.org/10.1109/jstars.2021.3088529.

Pane, L., Franceschi, E., De Nuccio, L., Carli, A., calorimetry, 2001. Applications of thermal analysis on the marine phytoplankton, Tetraselmis suecica. J. Therm. Anal. Calorim. 66 (1), 145–154. https://doi.org/10.1023/A:1012443800271.

Patrick, R., 1971. The effects of increasing light and temperature on the structure of diatom communities. Limnol. Oceanogr. 16 (2), 405–421. https://doi.org/10.4319/lo.1971.16.2.0405.

Poornima, E.H., Rajadurai, M., Rao, T.S., Anupkumar, B., Rajamohan, R., Narasimhan, S. V., Rao, V.N.R., Venugopalan, V.P., 2005. Impact of thermal discharge from a tropical coastal power plant on phytoplankton. J. Therm. Biol. 30 (4), 307–316. https://doi.org/10.1016/j.jtherbio.2005.01.004.

Poornima, E.H., Rajadurai, M., Rao, V.N.R., Narasimhan, S.V., Venugopalan, V.P., 2006. Use of coastal waters as condenser coolant in electric power plants: impact on phytoplankton and primary productivity. J. Therm. Biol. 31 (7), 556–564. https://doi.org/10.1016/j.jtherbio.2006.05.009.

Poornima, E.H., Rao, V.N.R., Venugopalan, V.P., 2012. Effects of Power Plant Entrainment on Phytoplankton, Operational and Environmental Consequences of Large Industrial Cooling Water Systems. Springer, pp. 315–337.

PRIS, 2021. https://www.nucnet.org/world-nuclear-map.

Rajagopal, S., Jenner, H.A., Venugopalan, V.P., 2012. Operational and Environmental Consequences of Large Industrial Cooling Water Systems. Springer, New York, pp. 319–323.

Richardson, T.L., Gibson, C.E., Heaney, S.I., 2008. Temperature, growth and seasonal succession of phytoplankton in Lake Baikal, Siberia. Freshw. Biol. 44 (3), 431–440. https://doi.org/10.1046/j.1365-2427.2000.00581.x.

Roemmich, D., McGowan, J., 1995. Sampling zooplankton: correction. Science 268 (5209), 352–353. https://doi.org/10.1126/science.268.5209.352-b.

Suresh, K., Ahamed, M.S., Durairaj, G., Nair, K.V.K., 1993. Impact of power plant heated effluent on the abundance of sedentary organisms, off Kalpakkam, East coast of India. Hydrobiologia 268 (2), 109–114. https://doi.org/10.1007/bf00006881.

Tang, S., Yan, Y., Chen, B., 2013. Impacts of thermal effluent on the phytoplankton community structures nearby Dayawan Nuclear Power Station in spring and summer. J. Appl. Oceanogr. 32 (3), 373–382. https://doi.org/10.3969/J.ISSN.2095-4972.2013.03.010.

Wang, G.L., Xiong, X.J., 2013. Distribution and variation of warm water discharge in the coastal area of tianwan. Adv. Mar. Sci. 31 (1), 69–74. https://doi.org/10.3969/j.issn.1671-6647.2013.01.008 (In Chinese).

Utermöhl, H., 1958. Zur Vervolkommung der quantitativen phytoplankton-Methodik. Methodik. Mitt. Int. Verein. Theor. Angew. Limnol. 9, 1–38. https://doi.org/10.1080/05384680.1958.11904091.

Wang, Y.J., Liu, D.Y., Lee, K., Dong, Z.J., Di, B.P., Wang, Y.Q., Zhang, J.J., 2017. Impact of Water-Sediment Regulation Scheme on seasonal and spatial variations of biogeochemical factors in the Yellow River estuary. Estuarine. Coast Shelf Sci. 198, 92–105. https://doi.org/10.1016/j.ecss.2017.09.005.

Wang, Y.B., Zhang, J.J., Wu, W.T., Liu, J., Ran, X.B., Zhang, A.J., et al., 2022. Variations in the marine seawater environment and the dominant factors in the Lianyungang coastal area. Reg. Stud. Mar. Sci. 52, 102276 https://doi.org/10.1016/j.rsma.2022.102276.

Wei, G., Wei, X., Liu, Y., Zhang, K., Teng, K., Wang, S., 2016. The current situations and problems in environmental assessment of thermal discharge from nuclear power plant in China. Sci. Technol. Rev. 15, 66–71. https://doi.org/10.3981/j.issn.1000-7857.2016.15.009 (In Chinese).

WNPR, 2022. World Nuclear Performance Report. https://www.world-nuclear.org/getmedia/9dafaf70-20c2-4c3f-ab80-f5024883d9da/World-Nuclear-Performance-Report-2022.pdf.aspx.

Xu, D., Wang, H., Han, D., Chen, A., Niu, Y., 2021. Phytoplankton community structural reshaping as response to the thermal effect of cooling water discharged from power plant. Environ. Pollut. 285, 117517 https://doi.org/10.1016/j.envpol.2021.117517.

Yang, C., Nan, J., Yu, H., Li, J., 2020. Embedded reservoir and constructed wetland for drinking water source protection: effects on nutrient removal and phytoplankton succession. J. Environ. Sci. 87 (1), 260–271. https://doi.org/10.1016/j.jes.2019.07.005.

Yu, J., Tang, D.L., Oh, I.S., Yao, L.J., 2007. Response of harmful algal blooms to environmental changes in daya bay, China. Terr. Atmos. Ocean Sci. 18 (5) https://doi.org/10.3319/TAO.2007.18.5.1011(Oc.

Yuan, Y., Su, J., 1984. Numerical modeling of the circulation in the east China sea. In: Ichiye, T. (Ed.), Ocean Hydrodynamics of the Japan and East China Seas, vol. 39. Elsevier Oceanography Series, pp. 167–176.

Zhang, C.Y., 2006. Effect and Analyss of Ocean Engineering on Ecologic Environment in Lianyungang Coastal Area. Master Thesis. Ocean university of China (In Chinese).

Zhang, J.J., Wang, Y.B., Wang, Y., Wang, T.T., M L Q, Gao, Y.J., Lü, Z.B., 2021. Effects of marine engineering construction on environmental factors and phytoplankton in the coastal area of Lianyungang. China Environ. Sci. 9 (41), 4253–4262. https://doi.org/10.3969/j.issn.1000-6923.2021.09.032 (In Chinese).

Zhang, S.W., Wang, Q.Y., Lü, Y., Cui, H., Yuan, Y.L., 2008. Observation of the seasonal evolution of the Yellow Sea cold water mass in 1996–1998. Continent. Shelf Res. 28, 442–457. https://doi.org/10.1016/j.csr.2007.10.002.

Zhang, X.F., Xu, J.P., Zhang, M.Q., Li, J., 2019. Distribution of thermal discharge from Tianwan nuclear power plant: analysis of thermal infrared data from landsat-8. Adv. Mar. Sci. 37 (3), 8. https://doi.org/10.3969/j.issn.1671-6647.2019 (In Chinese).

Zhao, H., Liu, Y., Song, M., Song, G., Ding, G., 2018. Influence of environmental factors on the growth of skeletonema costatum in the donggang red-tide-monitoring area of Liaoning. Environ. Dev. 30, 25–27 (In Chinese).

Zhu, X.Y., Xu, H.H., Xu, X., Ge, Y.H., Chen, P.P., Yang, H., 2017. Community composition of net-collected phytoplankton and its relation to environmental factors near Lianyungang sea area. J. Appl. Oceanogr. 36, 385–394. https://doi.org/10.3969/J.ISSN.2095-4972.2017.03.012 (In Chinese).